ARTICLE

Supplementary materials

Received 00th January 20xx,
Accepted 00th January 20xx

DOI: 10.1039/x0xx00000x

Temperature sensitive hydrogels cross-linked by magnetic Laponite RD®: Effects of particle magnetization

Nikolai I. Lebovka,*[a] Yurii M. Samchenko, Liudmyla O. Kernosenko, Tatiana P. Poltoratska, Natalia O. Pasmurtseva, Igor E. Mamyshev, Vladimir A. Gigiberiya

The work discusses the synthesis and the properties of magnetite modified Laponite® RD platelets (Lap). Magnetized Lap (mLap) nanoparticles were synthesized by a co-precipitation method with different weight ratios X= Fe_3O_4/Lap (=0-2). For characterization of the samples the particle size distributions and sedimentation behavior in an external magnetic field were studied. The temperature sensible hydrogels on the base of N-isopropylacrylamide) cross-linked by mLap were synthesized. An increased aggregation of mLap particles in aqueous suspensions has been revealed, but all the systems demonstrated high sedimentation stability. Significant effects of value of X on rate of sedimentation mLap particles in magnetic fields and on the swelling ability of hydrogels have been revealed. For example at X=2 the increase in swelling by ≈2.7 was observed as compared with swelling for hydrogels based on pure Lap.

[a] *Institute of Biocolloidal Chemistry named after F. D. Ovcharenko, NAS of Ukraine, 42, blvr. Vernadskogo, Kyiv 03142, Ukraine. E-mail:lebovka@gmail.com*

† Footnotes relating to the title and/or authors should appear here.
Electronic Supplementary Information (ESI) available: Experimental section and supplementary figures. See DOI: 10.1039/x0xx00000x

Structural formulas of some chemicals

Iron(II) sulfate heptahydrate $FeSO_4 \cdot 7H_20$ (Merck, 99%), iron(III) chloride $FeCl_3$ (Merck, 98%), ammonium $NH_3 \cdot H_2O$ (Merck, 25%), tetrasodium pyrophosphate $Na_4P_2O_7$ (TSPP, Merck, 95 %),ammonium persulfate $(NH_4)_2S_2O_8$, (APS, Sigma, 98%), N,N,N',N'-tetramethylenediamine, (TEMED, Merck, 99%), tetrasodium pyrophosphate (TSPP, Merck) were used as received without further purification. N-isopropylacrylamide, NIPAAm, (Sigma-Aldrich, 97%) was recrystallized from hexane and dried under vacuum. Structural formulas of some chemicals used this paper are presented in Table S1.

Table S1. Structural formulas of some chemicals

Formula	Name and short description
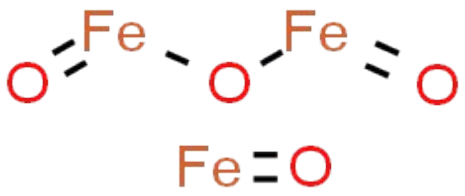	Magnetite, Fe_3O_4 ($FeO \cdot Fe_2O_3$) Iron (II, III) oxide structure Molar mass: 231.533 g/mol Density: 5.17 g/cm³ Melting point: 1597 °C
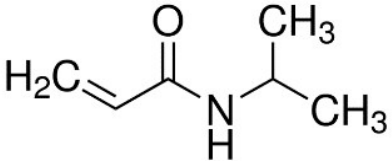	N-isopropylacrylamide (NIPAAm) is a monomer for polymerization. It forms a hydrogel when cross-linked with N,N'-methylene-bis-acrylamide (MBAm) or N,N'-cystamine-bis-acrylamide (CBAm). It expels its liquid contents at a temperature near 32°C. Density: 1.1 g/cm³ Melting point 96 °C
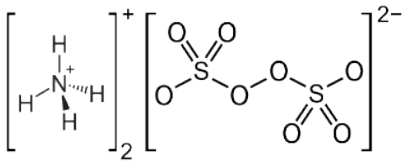	Ammonium persulfate $(NH_4)_2S_2O_8$ (APS) is an oxidizing agent and a radical initiators in the polymerization of AA. It is used in polymer chemistry, as an etchant, and as a cleaning andbleaching agent. Molar mass: 228.18 g/mol Density: 1.98 g/cm³
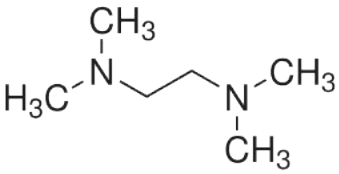	N,N,N',N'-tetramethylenediamine (TEMED) is used with APS to catalyze the polymerization of NIPAAm. Molar mass116.208 g/mol Density0.7765 g/cm³ Melting point −58.6 °C
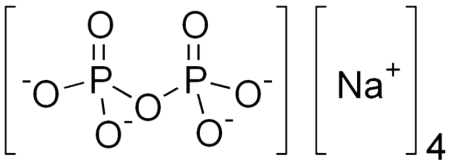	Tetrasodium pyrophosphate (TSPP) is a buffering and dispersing agent. Common foods containing tetrasodium pyrophosphate include chicken nuggets, marshmallows. In toothpaste and dental floss, tetrasodium pyrophosphate acts as a tartar control agent. Molar mass265.9 g/mol Density2.534 g/cm³ Melting point 988 °C

Fourier transform infrared (FTIR) spectroscopy studies on Lap, magnetite and Lap-magnetite nanocomposites

FTIR analysis was carried out using a spectrometer IR Affinity-1S (Shimadzu, Japan) using an attenuated total reflection technique (internal reflection spectroscopy) in the spectral range 400–4000 cm^{-1} with a resolution of 2 cm^{-1} and accumulations of 128 scans which were combined to average out random absorption artifacts. KBr pressed disk technique was used. Pellets were prepared using the standard technique under a pressure of 15 ton/cm^2 with a barrel 16 mm in diameter. The positions of the absorptions appearing in the spectra as shoulders were determined by second derivative.

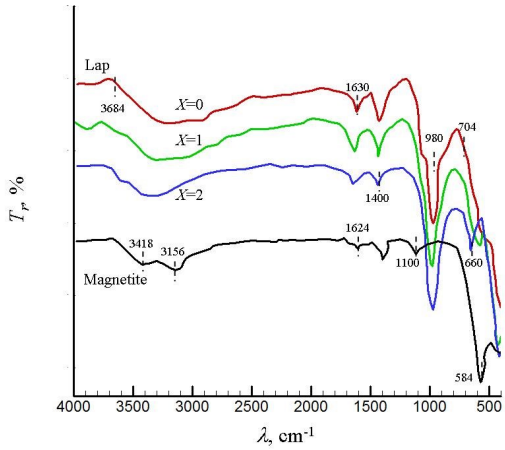

Fig. S1. FTIR spectra (transmission, T_r, versus wavenumbers, λ, of pristine Lap (X=0), mLap (X=1 and X=2) and magnetite samples.

Figure S1 shows FTIR spectra for Lap (X=0), mLap (X=1 and X=2) and magnetite samples. The assignment of band is presented in Table S2. The broad bands in the interval between 3000-3500 cm-1, and bands near 1630 and 1400 cm^{-1} correspond to the OH stretching vibrations of H_2O molecules adsorbed on samples. These bands were observed for all samples. For pristine Lap sample the very characteristic is an intense band at the wavelengths between 980-1010 cm-1 that corresponds to the Si–O and Al-0-H stretching vibrations of the tetrahedral sheets. For pure magnetite sample the intensive bands at 584 cm-1 and 1100 cm-1 correspond to the different vibration modes in the bond Fe-OH. In magnetized samples mLap the both bands corresponding to the Lap at ≈ 980 cm^{-1} and magnetite at ≈ 660 cm^{-1} were only observed at sufficiently high content of magnetite (X≥2). The noticeable shift of the Fe-O vibration band of magnetite may reflect strong interactions between Fe3O4 and Lap species in magnetized mLap samples.

Table S2

The assignment of the bands observed in FTIR spectra of Lap and magnetite samples.

Position, cm^{-1}	Assignment
≈3450, 1630, 1400	OH stretching vibrations of H_2O molecules adsorbed on both nanoparticles and KBr used for IR measurement
Lap(Pálková et al. 2010)	
3684	Stretching (ν) vibrations of Mg_3OH groups
3645	Valence fluctuations of surface hydroxyl groups
980-1010	Si–O stretching vibrations of the tetrahedral sheets
704	O_b–Si–O_{ap} bending vibration, i.e. vibration involving basal bridging oxygen's (O_b) and apical non-bridging oxygen's (O_{ap}).
Magnetite (Morales et al. 1999; Manuel et al. 2008; El-Mahdy et al. 2014)	
3126	–OH vibration
1100	Fe-O asymmetric vibration in the bond Fe-OH.
584, 637 cm−1	Stretching and torsional vibration modes of the Fe–O bonds of the magnetite

Thermogravimetric analysis (TGA) of Lap, magnetite and Lap-magnetite nanocomposites

TGA and DTA studies of the samples were performed using a Q-1000 derivatograph (MOM, Hungary) equipped with a data logger.

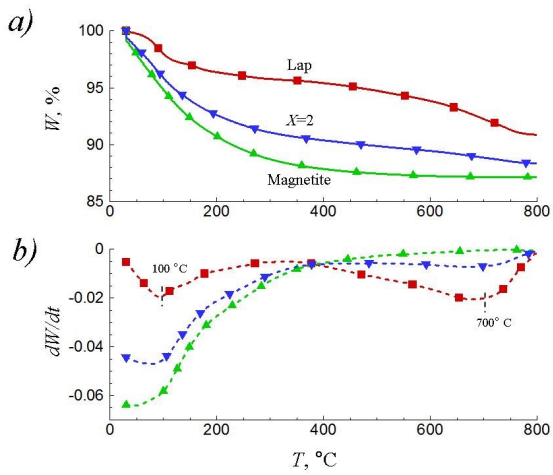

Fig. S2. Thermograms presented as relative weight W (a) and derivative dW/dT (b) versus the temperature T of pristine Lap (X=0), mLap (X=2) and magnetite samples.

The studies were carried out in the dynamic mode in air, in the temperature range of 293–1273 K, at the heating rate of 10° C/min from 25 to 800°C. Samples (40 mg) were placed in a conic platinum crucible.

Figure S2 shows TGA curves for pristine Lap (*X*=0), mLap (*X*=2) and magnetite samples. Pristine Lap (X=0) demonstrated two thermal decomposition steps corresponding to the loss of adsorbed water (≈100 °C) and the dehydroxylation of the Lap (≈700 °C). Total weight loss of Lap at *T*=800 °C was approximately 9 % Observed phase-transition temperatures obtained in this study were in reasonable agreement with those reported in literature for nanoparticles of Lap (Wang et al. 2009). Hydrid sample (*X*=2) also demonstrated the step related with the loss of adsorbed water. For pure magnetite mass losses observed at ≈ 100° C corresponds to the removal of physically adsorbed water. The differential thermal analysis (DTA) studies also revealed exothermic peaks at *T*≈554° C attributed to phase transitions of magnetite into hematite phase (Chen 2013).

References

Chen Y-H (2013) Thermal properties of nanocrystalline goethite, magnetite, and maghemite. J Alloys Compd 553:194–198

El-Mahdy GA, Atta AM, Al-Lohedan HA (2014) Synthesis and evaluation of poly (sodium 2-acrylamido-2-methylpropane sulfonate-co-styrene)/magnetite nanoparticle composites as corrosion inhibitors for steel. Molecules 19:1713–1731

Manuel J, Kim J-K, Ahn J-H, et al (2008) Surface-modified maghemite as the cathode material for lithium batteries. J Power Sources 184:527–531

Morales M d P, Veintemillas-Verdaguer S, Montero MI, et al (1999) Surface and internal spin canting in γ-Fe2O3 nanoparticles. Chem Mater 11:3058–3064

Pálková H, Madejová J, Zimowska M, Serwicka EM (2010) Laponite-derived porous clay heterostructures: II. FTIR study of the structure evolution. Microporous Mesoporous Mater 127:237–244

Wang B, Zhou M, Rozynek Z, Fossum JO (2009) Electrorheological properties of organically modified nanolayered laponite: influence of intercalation, adsorption and wettability. J Mater Chem 19:1816–1828